Spectral line commissioning S-band - Part I: S4 low-resolution tests, 32k broadband mode

Michael Rugel, Arshia Jacob, Sarrvesh Sridhar, Olaf Wucknitz,
Andreas Brunthaler, Friedrich Wyrowski, Karl M. Menten,
Su Ann Mao, Hans-Rainer Kloeckner

April 21, 2022

Scientific background: We present commissioning observations to test the capability of the S-band receiver system for spectral line observations of the three CH hyperfine-structure (hfs) transitions of CH at 3.3 GHz. Though expected to be generally quite weak, the CH radio lines are a promising probe of the molecular interstellar medium in a variety of physical conditions (e.g., Rydbeck et al. 1973; Genzel et al. 1979), but subject to complex excitation mechanisms which have been studied in a recent project with the JVLA in combination with SOFIA (Jacob et al. 2021). Further observations in the Southern hemisphere are planned as potential part of commensal observations with the S-band receivers on the MeerKAT telescopes within the MeerKAT Galactic Plane Survey (MGPS; Padmanabh et al. 2020), which is lead by the Max Planck Institute for Radio Astronomy in Bonn, Germany. We select three strong cm continuum sources of which we expect emission profiles which are typical for Galactic CH, showing both strong emission associated with giant molecular clouds and weak components from molecular gas along the line of sight. All three sources – Sgr B2, G09.622+0.19 and W51 – are sites of on-going star formation. Two of the three sources have been part of the aforementioned JVLA program lead by Arshia Jacob (Jacob et al. 2021), such that we have a direct reference data set at hand (figure 2, Jacob et al. 2021), to which we will be comparing the commissioning CH emission line profiles obtained with MeerKAT.

Objectives: To test the applicability of the narrowband mode in the S4 band for observations of the three hfs transitions of the CH ground state at 3.3 GHz. We checked for potential saturation of the receiver and tested the bandpass stability. We compared the data to previous observations with the JVLA (Jacob et al. 2021).

Table 1: Spectroscopic properties of the CH ground state hyperfine-structure transitions. The columns are (from left to right): the transition as described by the hyperfine quantum number (F), the frequency of the transition, the Einstein A coefficient and the relative line intensities at LTE. The CH frequencies were measured by Truppe et al. (2014) with uncertainties of 3 Hz.

Transition $F' - F''$	Frequency [MHz]	A_E $\times 10^{-10}$ [s^{-1}]	Relative Intensity
CH $0^- - 1^+$	3263.793447	2.876	1.0
CH $1^- - 1^+$	3335.479356	2.045	2.0
CH $1^- - 0^+$	3349.192556	1.036	1.0

Table 2: Source list for the MeerKAT CH commissioning

Source name	GLON [deg]	GLAT [deg]	RA h:m:s	Dec °:′:″	Vel km s^{-1}	$\sigma(0^- - 1^+)$ mJy $beam^{-1}$	$\sigma(1^- - 1^+)$ mJy $beam^{-1}$	$\sigma(1^- - 0^+)$ mJy $beam^{-1}$
Sgr B2M	0.67	-0.04	+17:47:20.5	-28:23:06	64.0	5.8	4.9	5.0
G09.622+0.19	9.62	0.19	+18:06:14.9	-20:31:37	4.3	4.0	3.3	3.4
W51	49.49	-0.39	+19:23:43.9	+14:30:31	62.0	5.5	4.9	4.9

Observations and data reduction: We tested the broadband correlator mode in the S4 band with 32k channels, which covers the three CH lines with a native channel width of 27.703 kHz (~2.4 km s^{-1}). The observations were conducted on September 16, 2021 by Sarah Buchner. The observing band was centered at 3062.5 MHz with a dump time of 8s. Sgr B2, G09.622+0.19 and W51 were observed for 10 min each. For flux and bandpass calibration, J1939-6342 was observed twice for 5 min each. To test the bandpass stability, the two scans were separated by 30 min. For calibration of the complex gains, we used short scans of J1733-1304 and J2011-0644. To make the observations usable also for continuum polarization observations, we observed J1331+3030 (3C286) at the beginning of the observations for ~10min.

The data are downloaded as measurement tar file. As we are only interested in selected spectral lines, we reduce the data size by creating a new measurement set that only contains channels within a range of ±300 km s^{-1} around each of the CH transitions as three separate spectral windows. For calibration, we use the CASA-based calibration pipeline from the MGPS survey (S. Sridhar) with CASA version 5.7.2. Antenna m000 was chosen as reference antenna. Both linear polarizations were averaged for the derivation of the flux scale. The flux scale is determined from J1939-6342, using the Steven-Reynolds 2016 model. We flag antennas m025, m031, m054 and m056, and apply automatic flagging (`tfcrop`).

The continuum is subtracted in the visibility plane from line-free channels. The data is imaged using tclean in CASA 6.4.3. We limit the visibilties to the inner core by imposing a selection in the uv-plane between 0.5-10 kλ, and using Briggs weighting with robust=0. This leads to an increase in the noise, but brings the data closer to the angular resolution of the JVLA data and improves the shape of the point-spread function. We choose the native channel width for imaging and 5″ pixels. The correction and interpolation of the spectral axes to the local standard of rest are done automatically in tclean.

In the following, we consider the CH hyperfine-structure lines for W51 and Sgr B2, as the transitions (in particular at 3.264 GHz) are the strongest for these two objects. The restoring beams are 25″×18″ for W51, and 21″ × 16″ for Sgr B2. To compare the MeerKAT commissioning observations for CH with the JVLA data from Jacob et al. (2021), we smooth the MeerKAT S-band data to 23″ and 27.″76 for Sgr B2 and W51, respectively. The JVLA data is gridded onto the MeerKAT coordinate raster and the spectral resolution degraded to the MeerKAT spectral resolution (~2.4 km s^{-1}).

Although not the main focus of this report, for SgrB2, we further compared the spectra of two hydrogen radio recombination lines, H130α (3491.258 MHz) and H123α (2959.033 MHz), which also have been observed with the JVLA (A. Jacob, priv. comm.). The data processing steps were similar as for the CH transitions, only that we chose to smooth all data to a common resolution of 50″.

Results:

Applicability of the narrowband mode at S4 As this mode was not available at the time of the observations, we were not able to conduct these tests. These commissioning observations need to be delayed to when this telescope mode becomes available.

Bandpass stability for weak spectral line observations at S4 band On the short interval of 30 min, the bandpass appears to be stable within the noise level of (Fig. 1). Visual monitoring of the correlator levels showed that the backend did not saturate for strong sources such as Sgr B2 and W51, likely due to the high channel number of 32k.

The sensitivities of the data cubes are listed in Table 2, and have been determined as median of the standard deviation in all channels and have been evaluated before degrading the data to the common resolution with the VLA data. Assuming values for the $SEFD$ around 400–500 Jy, we estimate the theoretical noise in a spectral channel to be between ~2.8 mJy beam^{-1} and ~3.5 mJy beam^{-1} considering 52 antennas. For the CH $1^- - 1^+$ and $1^- - 0^+$ lines at 3335.5 and 3349.2 GHz, respectively, the measured noise agrees well with the theoretical estimates for source G09.622+0.19. We note that the data cubes have been created with a lower number of baselines due to the uv-range selection, which may lead to higher noise values. For all sources, the noise is 10–20 % larger for the CH $0^- - 1^+$ transition at 3263.8 GHz than for the other two CH transitions, which can be explained by an increase of $SEFD$ curve in this part of the frequency coverage. For SgrB2 and W51, we find elevated noise values, which are likely due to significant contributions of the continuum source temperature to the overall noise temperature: Estimating the continuum temperature from the 11 cm Effelsberg survey

(Reich et al. 1984, 1990), we find values of ∼19 K and 14 K for Sgr B2 and W51, respectively, compared to 4 K for G09.622+0.19. Additionally, W51 was observed at low elevations (elevation=22°), for which ground contributions to the system temperature may have become more significant as well.

Comparison to previous JVLA observations Figure 2 shows the CH transitions for the sources Sgr B2 and W51. All spectra were extracted from the peak of the continuum. We compare the MeerKAT to the JVLA observations and show both the smoothed and un-smoothed JVLA data, as well as the difference between the MeerKAT and the smoothed JVLA data.

We note generally very good agreement between all features: For Sgr B2, all three CH transitions agree with the JVLA measurements within 3σ. Especially the strongest transition, the CH line at 3263.8 MHz (see Table 1 for an overview) matches the JVLA observations well. For W51 (observed at very low elevations of 22°), the agreement is similarly well, except for the transition at 3263.8 MHz, for which one of the two peaks appears significantly stronger in the MeerKAT data. The strongest feature is not spectrally resolved at the resolution of the MeerKAT data, which may cause slight discrepancies. The integrated emission, however, differs between 10–15 % for both emission features, which may be due to slight calibration differences between the MeerKAT and VLA datasets. Good agreement between the MeerKAT and JVLA data is found for the H123α and H130α radio recombination lines for Sgr B2 (Fig. 3), which only deviate slightly for a very small amount of channels.

To quantify the agreement of the spectral axis, in Fig. 4 we show the cross-correlation of the MeerKAT and JVLA data for different velocity differences. We find that for all transitions in SgrB2 and W51, the cross-correlation function is centrally peaked at a velocity difference of $0\,\mathrm{km\,s^{-1}}$. This indicates that the spectral axes are well aligned.

Lastly, we note that the spectral resolution of $2.4\,\mathrm{km\,s^{-1}}$ is not sufficient to spectrally resolve many of the more narrow emission features (Fig. 2). To properly observe the CH lines, higher spectral resolution is needed. For observations of radio recombination lines, the spectral resolution of the broadband 32k-channel mode is sufficient (Fig. 3).

Conclusions We tested the S-band system for observations of CH and find that the data are in good agreement with previous observations with the JVLA. We note that for CH, better spectral resolution is necessary, which will only become available with the narrowband 107 MHz/53.5 MHz F-engine modes. The broadband 32k mode is an option for broader spectral lines and provides sufficient sampling for lines with line widths $\gtrsim 10\,\mathrm{km\,s^{-1}}$. We compare the bandpass between two scans separated by 30min and do not find significant variations.

References

Genzel, R., Downes, D., Pauls, T., Wilson, T. L., & Bieging, J. 1979, A&A, 73, 253

Jacob, A. M., Menten, K. M., Wiesemeyer, H., & Ortiz-León, G. N. 2021, A&A, 650, A133

Padmanabh, P. V., Barr, E. D., Mao, S. A., et al. 2020, The MeerKAT S-Band Galactic Plane Survey, Tech. rep., Max-Planck-Institut für Radioastronomie

Reich, W., Fuerst, E., Haslam, C. G. T., Steffen, P., & Reif, K. 1984, A&AS, 58, 197

Reich, W., Fuerst, E., Reich, P., & Reif, K. 1990, A&AS, 85, 633

Rydbeck, O. E. H., Elldér, J., & Irvine, W. M. 1973, Nature, 246, 466

Truppe, S., Hendricks, R. J., Hinds, E. A., & Tarbutt, M. R. 2014, ApJ, 780, 71

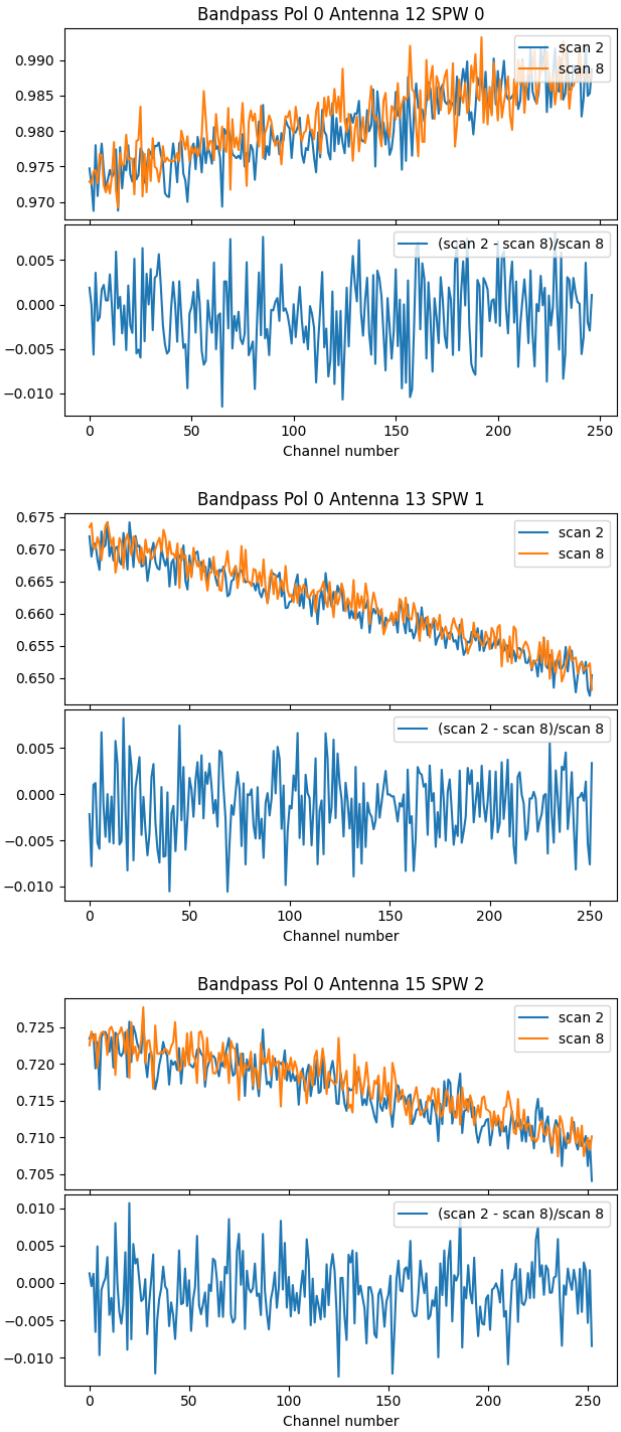

Figure 1: Bandpass solution for one polarization derived from two different scans of J1939-6342, separated by 30min. The lower panel in each plot shows the normalized difference. The different plots show the ranges around all three CH lines, for different antennae each.

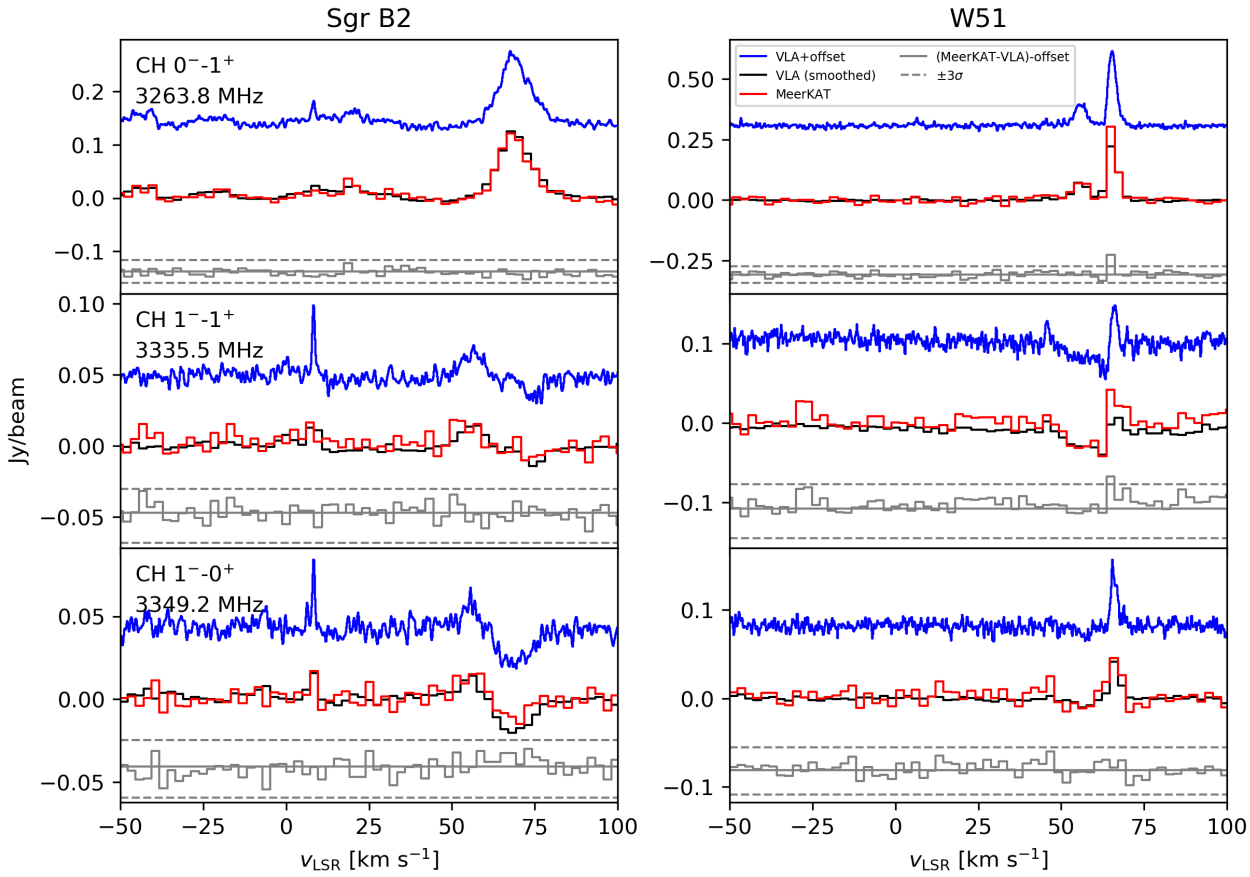

Figure 2: Comparison of the CH transition observed with the MeerKAT S-band receiver in S4 band (red) and with the JVLA (Jacob et al. 2021) (black, smoothed to the spectral resolution of the MeerKAT broadband observations). The JVLA data are also shown in their original spectral resolution (blue), indicating that high spectral resolution is needed to resolve narrow CH emission features. The difference between the MeerKAT and smoothed JVLA data is shown in gray together with 3σ levels.

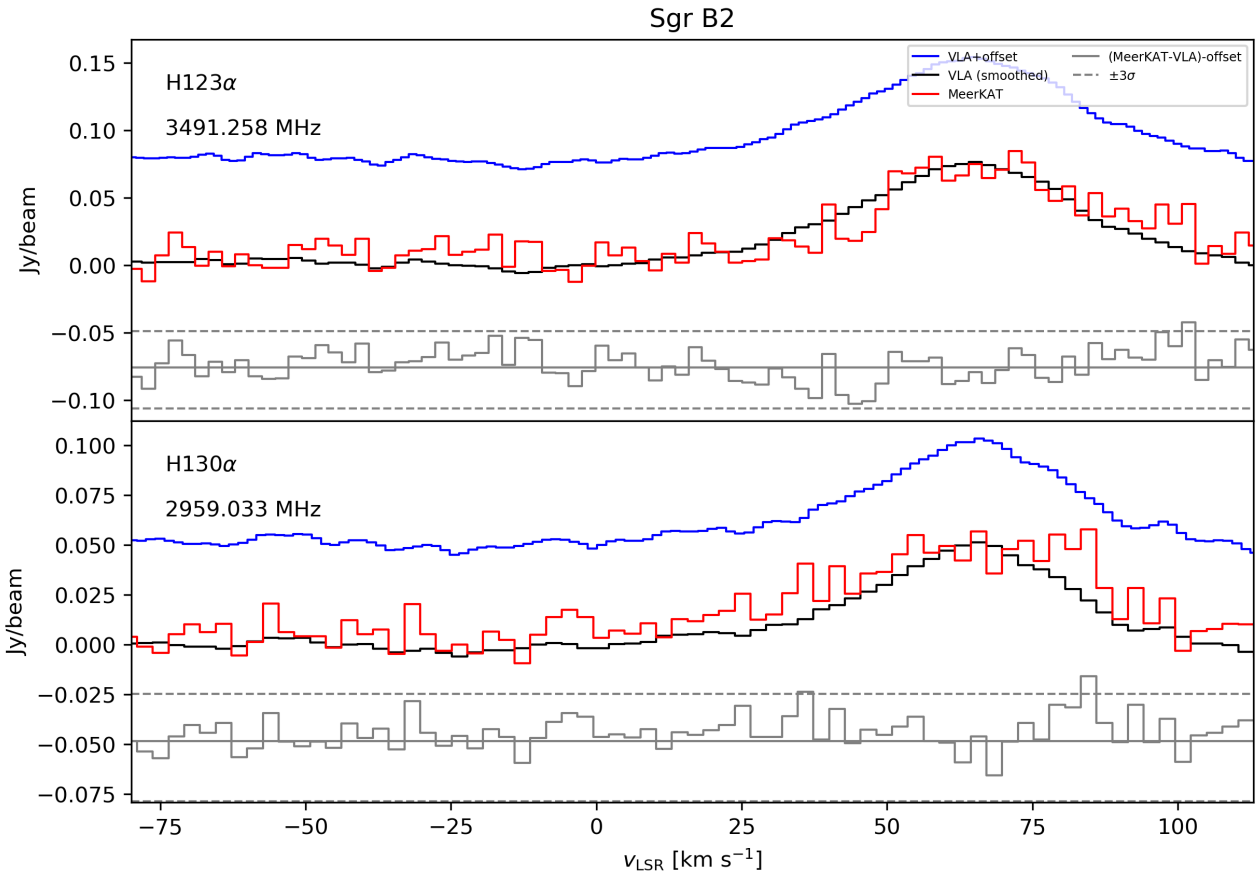

Figure 3: Comparison of the H130α and H123α transition for SgrB2 observed with the MeerKAT S-band receiver in S4 band and with the JVLA (Jacob et al. 2021). Spectra and colors as in Fig. 2.

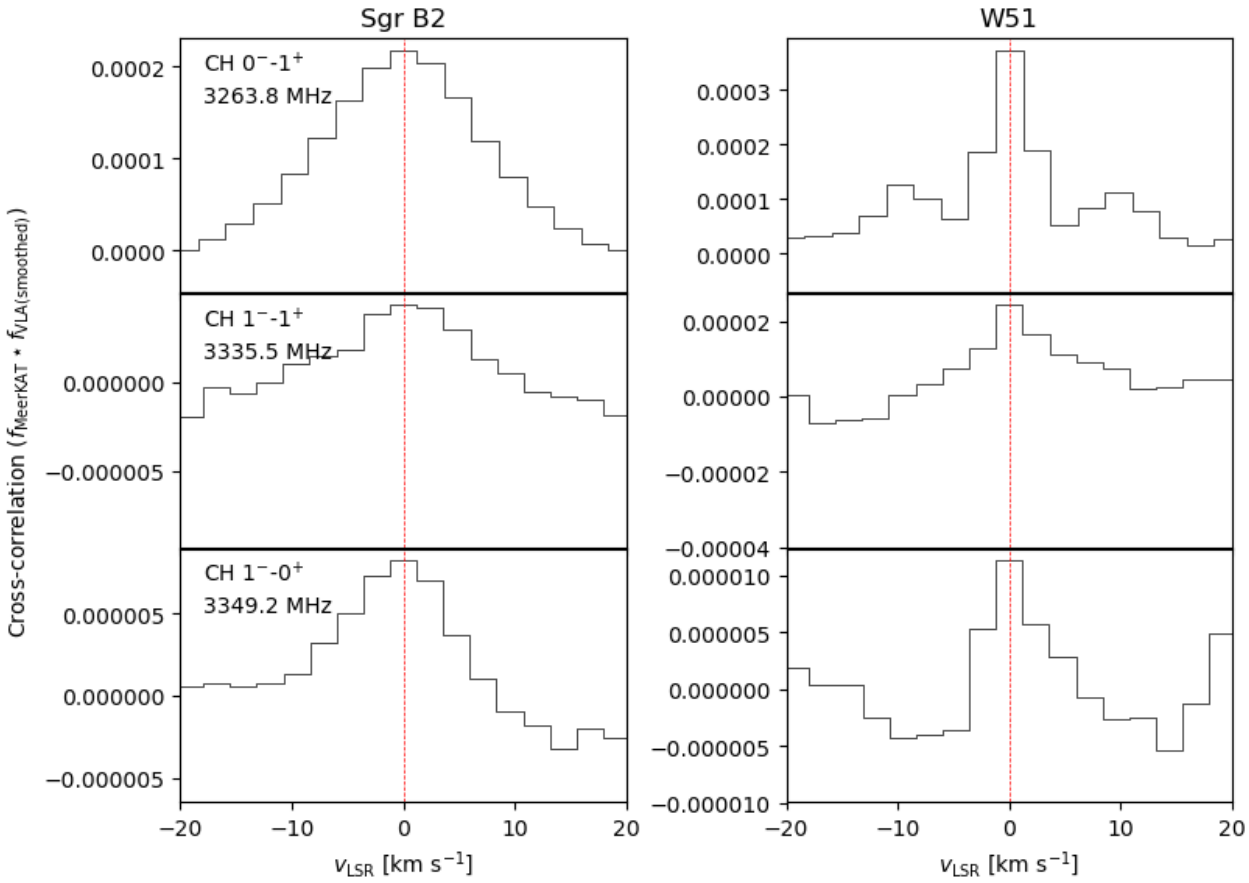

Figure 4: Cross-correlation of the CH transition observed with the MeerKAT S-band receiver in S4 band and with the JVLA (Jacob et al. 2021). The JVLA data have been smoothed the spectral resolution of the MeerKAT data. The dashed red line indicates no velocity shift.